UNIVERSITÀ DEGLI STUDI FIRENZE
DIEF DIPARTIMENTO DI INGEGNERIA INDUSTRIALE

ADDITIVE 4 BIOMEDICAL

October 17th–18th, 2022

MANUFACTURABILITY OF FUNCTIONALLY GRADED POROUS β-TI21S INNOVATIVE ARCHITECTED CELLULAR STRUCTURES PRODUCED BY LASER POWDER BED FUSION

Lorena Emanuelli

Plesso Didattico Morgagni, Viale Morgagni, 44-48, 50134 Firenze

CoCo AM SC 09/A3 Additive Manufacturing

ADM ASSOCIAZIONE NAZIONALE DISEGNO E METODI

COMET

aias

Introduction

- Titanium and its alloys
- Cellular structures
- Graded porosity
- Bone-implant connection improvement

Material

- Specimen design
- Powder composition
- Laser Powder Bed Fusion

Results

- 3D-Metrology
- CAD vs μ-CT
- Microstructural char.
- Mechanical char.

Conclusions

TITANIUM AND ITS ALLOYS

ADDITIVE 4 BIOMEDICAL

Material	Standard	E (GPa)	Tensile strength (MPa)	Alloy type
First generation biomaterials (1950 – 1990)				
Pure Ti Cp grade 1-4	ASTM 1341	100	240 - 550	a
Ti-6Al-4V ELI wrought	ASTM F136	110	860 - 965	a + b
Ti-6Al-4V ELI standard grade	ASTM F1472	112	895 - 930	a + b
Ti-6Al-7Nb wrought	ASTM F1295	110	900 - 1050	a + b
Second generation biomaterials (1990 – till date)				
Ti-15Mo-5Zr-3Al	ISO 5832-14:2019	80	900	b
Ti-13Nb-13Zr Wrought	ASTM F1713	79-84	973-1037	b
Ti-12Mo-6Zr-2Fe	ASTM F1813	74-85	1060 – 1100	b
Ti-35Nb-7Zr-5Ta		55	596	b
Ti-29Nb-13Ta-4.6Zr		65	911	b
Ti-35Nb-5Ta-7Zr-0.40		66	1010	b
Ti-15Mo-5Zr-3Al		82		b
Ti-15Mo-3Nb-3Al-0.2Si (Ti21S)		**52**	**830**	**b**

Human bone	Elastic modulus (GPa)
Cortical	17 – 20 (longitudinal) 6 – 13 (Transverse)
Cancellous	0.076 – 4

Too high elastic moduli comparing with the human bone

⇩

Design of cellular structures

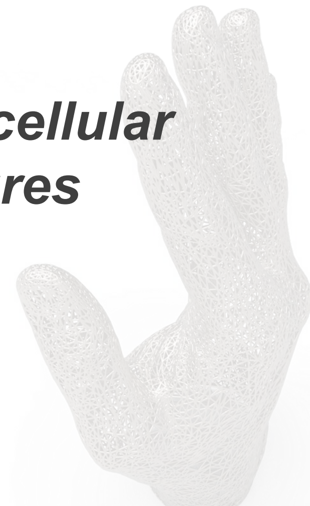

Low %Al , no V

Lowest E, good strength

No heat treatment

CELLULAR STRUCTURE

Strut-based lattices

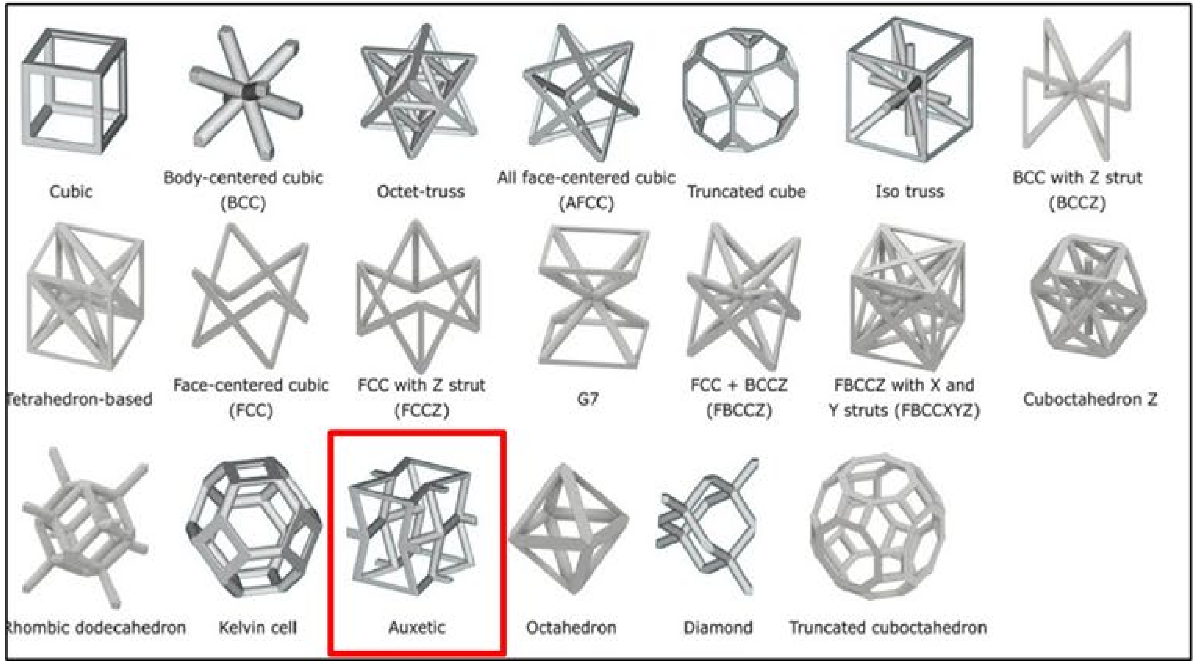

Triply periodic minimal surface

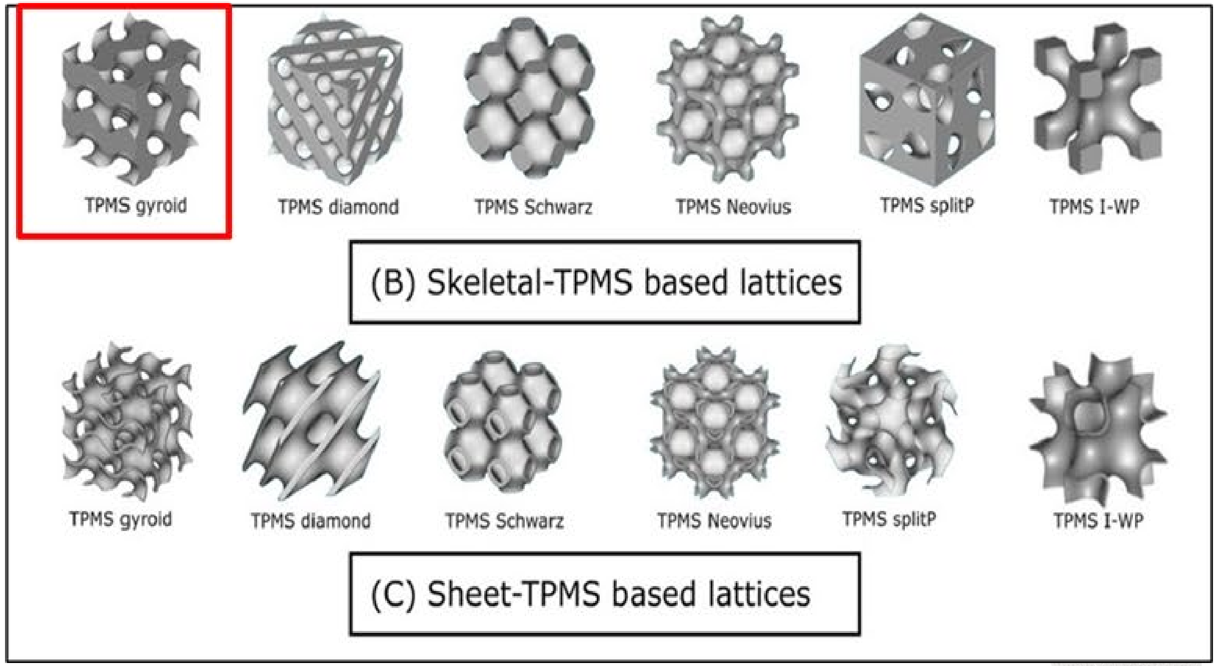

[Mater. Sci. Eng. R Reports. 144 (2021) 100606]

CELLULAR STRUCTURE

Strut-based lattices

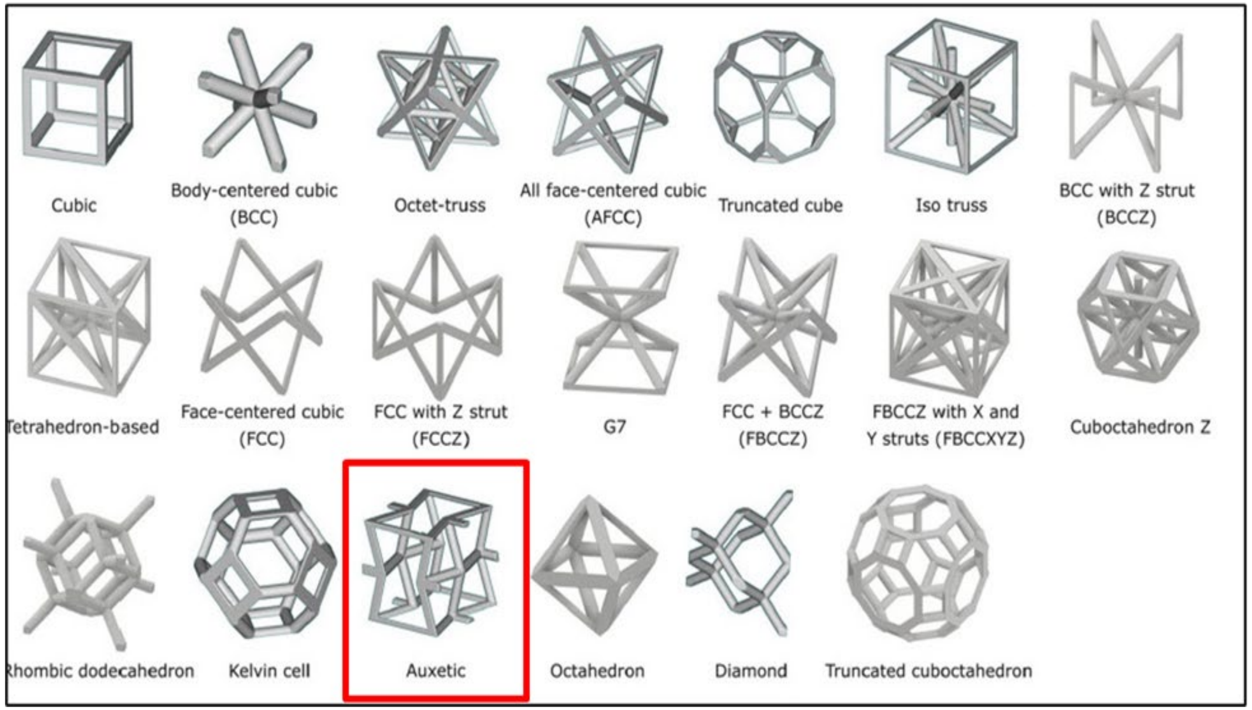

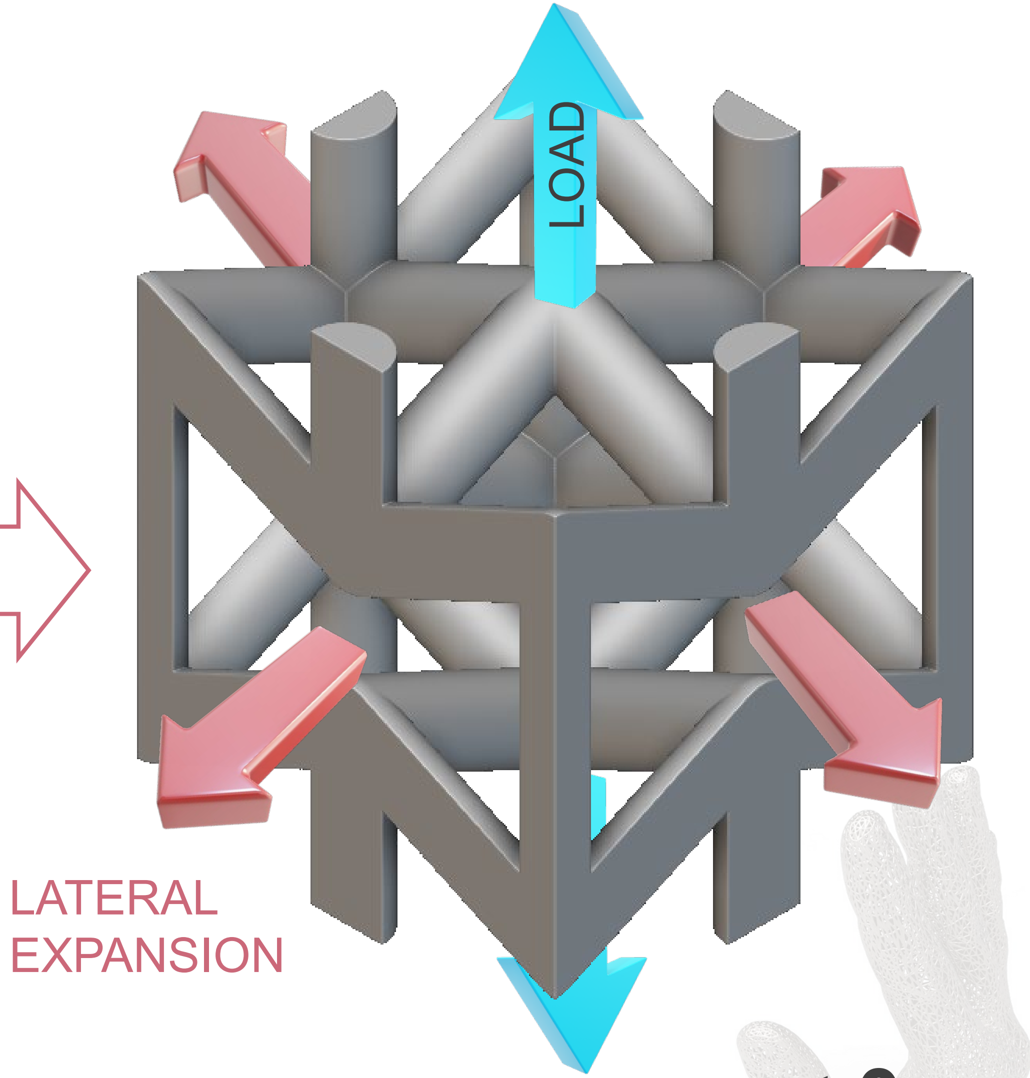

Auxetic structure $\nu < 0$

[Mater. Sci. Eng. R Reports. 144 (2021) 100606]

CELLULAR STRUCTURE

Triply periodic minimal surface

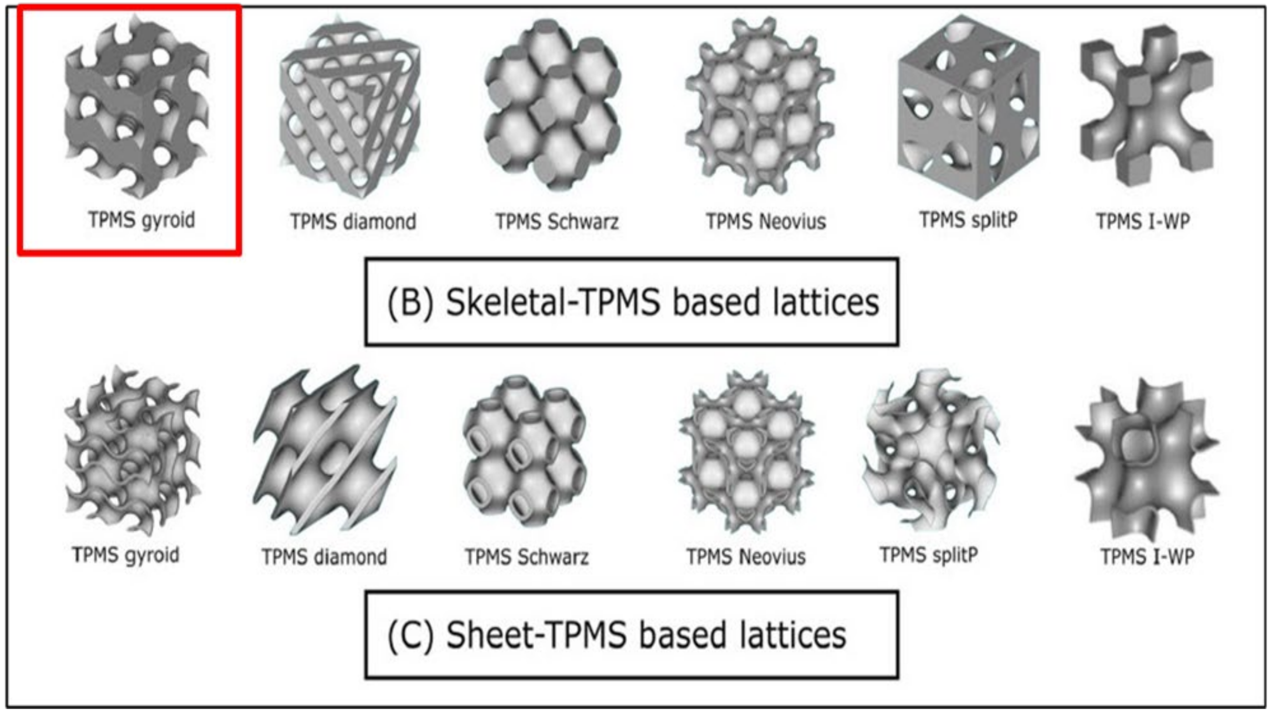

- $\nu > 0$
- Zero value of mean curvature at each point: no stress intensification
- Skeletal TPMS based structure is characterized by interconnected porosity and a lower elastic modulus respect to the sheet TPMS

[Mater. Sci. Eng. R Reports. 144 (2021) 100606]

GRADED POROSITY

Human bone porous structure

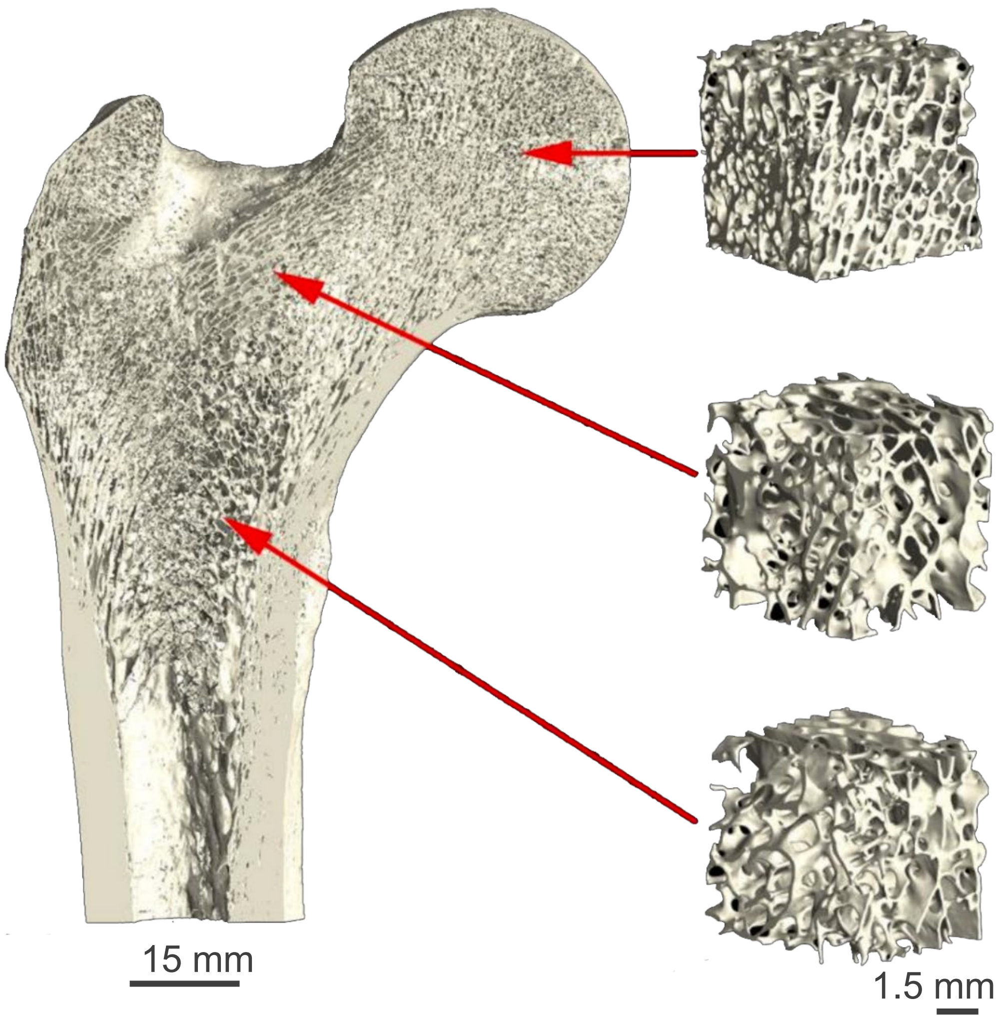

Functionally graded porous structure (FGPS)

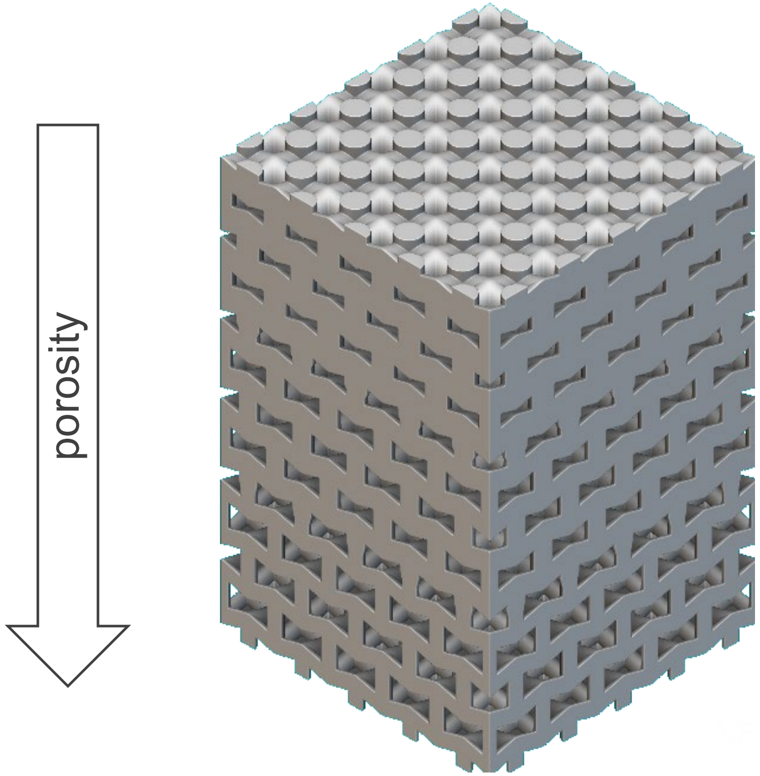

- Mimic the human bone porous structure
- Connection between porous structure and solid part

[Titanium for Consumer Applications Real World Use of Titanium (2019) 197-233]

BONE- IMPLANT CONNECTION IMPROVEMENT

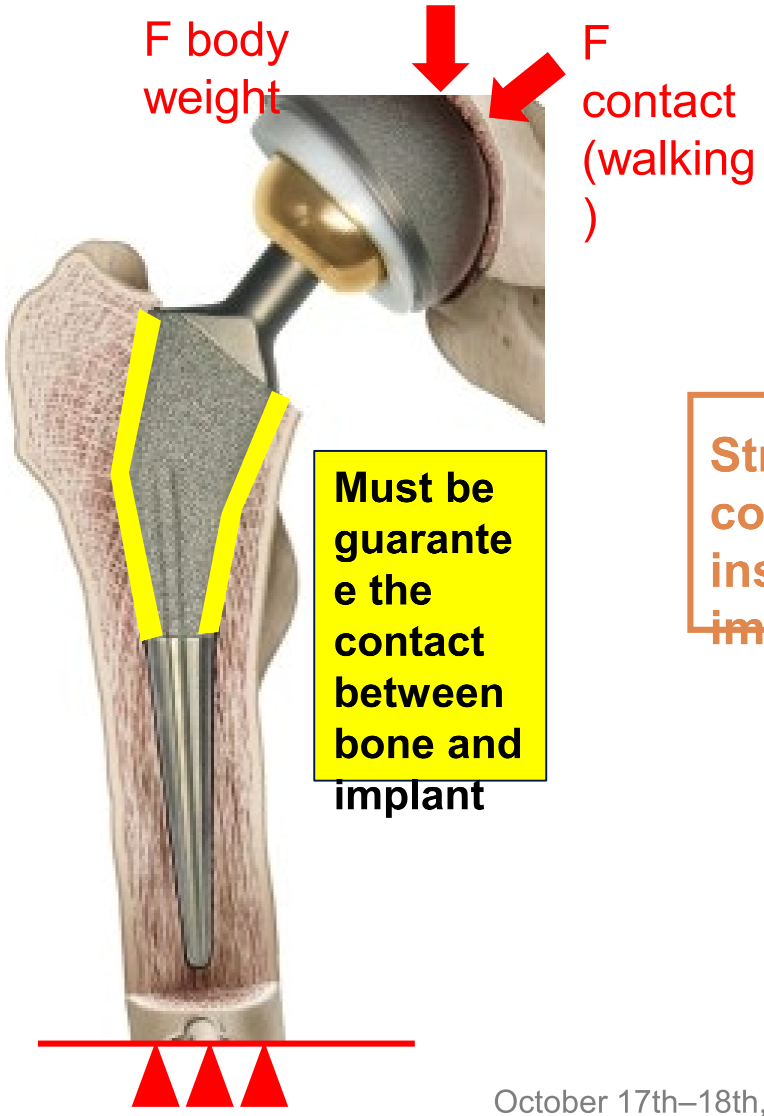

Must be guarantee the contact between bone and implant

Stress conditions inside porous implant part

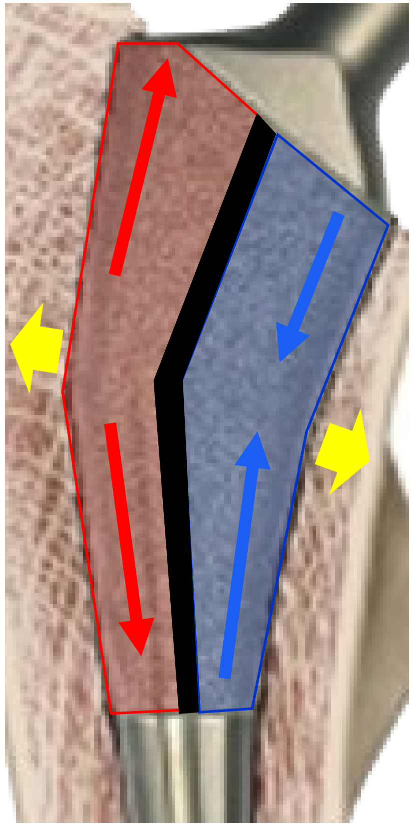

TENSILE STRESS

Auxetic structure to guarantee lateral expansion

COMPRESSION STRESS

TPMS structure to guarantee lateral expansion

FGP to promote connection with solid part and optimized pore size for osseointegration and mechanical performances

https://www.joint-surgeon.com/orthopedic-services/osteoarthritis-of-the-hip/total-hip-replacement

Material

SPECIMEN DESIGN

ADDITIVE 4 BIOMEDICAL

Auxetic unit cell

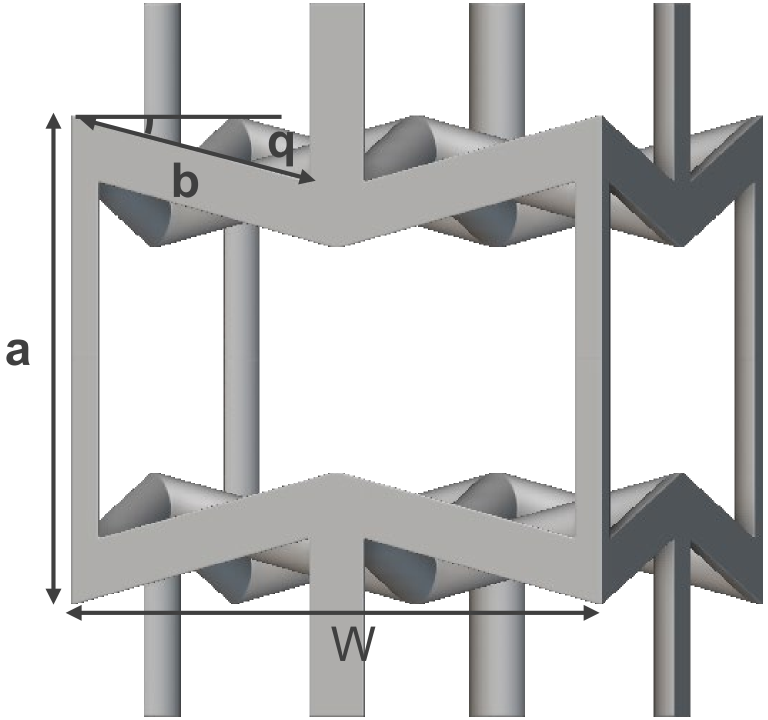

Aspect ratio a/b = 1.5

W = 4 mm

Design by nTopology software

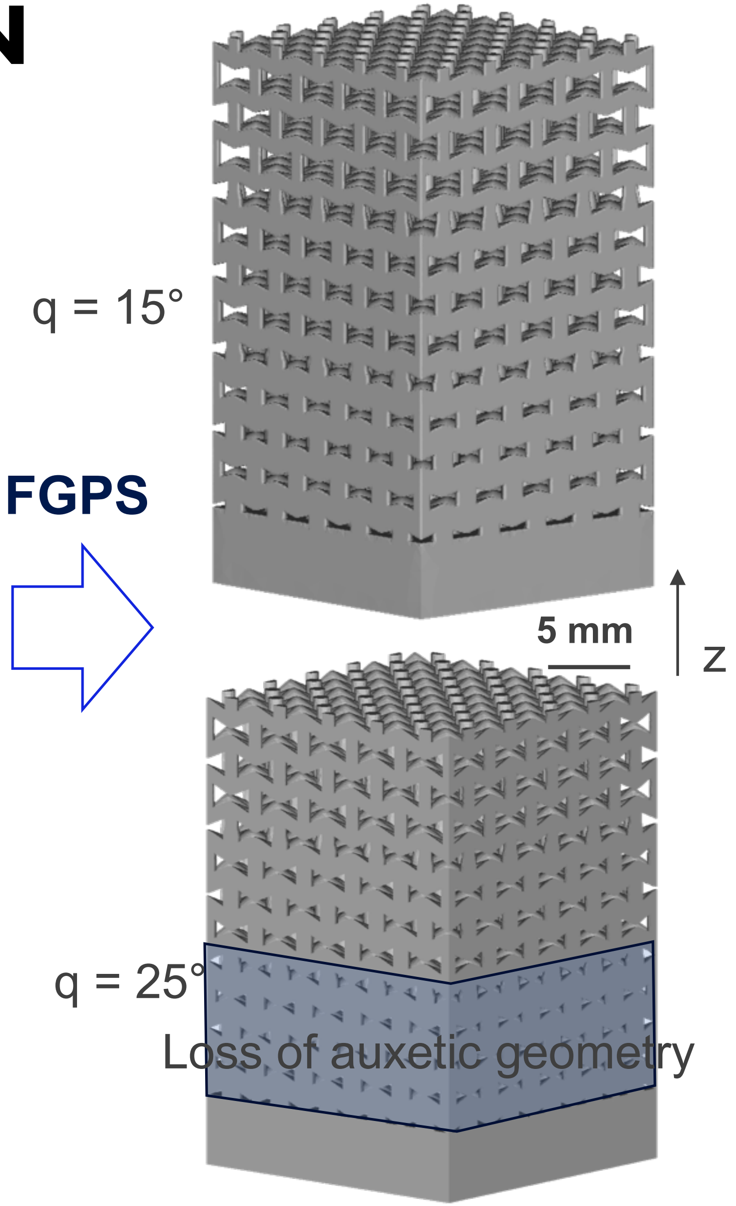

Relative density - dr (-)	Nominal strut thickness (mm)
0.34	1.10
0.49	1.38
0.66	1.68

3 auxetic unit cells for each density level along z axis

Relative density - dr (-)	Nominal strut thickness (mm)
0.40	1.10
0.58	1.38
0.75	1.68

Material

SPECIMEN DESIGN

$$G = \cos\left(\frac{2\pi x}{L}\right)\sin\left(\frac{2\pi y}{L}\right) + \cos\left(\frac{2\pi y}{L}\right)\sin\left(\frac{2\pi z}{L}\right) + \cos\left(\frac{2\pi z}{L}\right)\sin\left(\frac{2\pi x}{L}\right) - t = 0$$

Skeletal TPMS gyroid unit cell

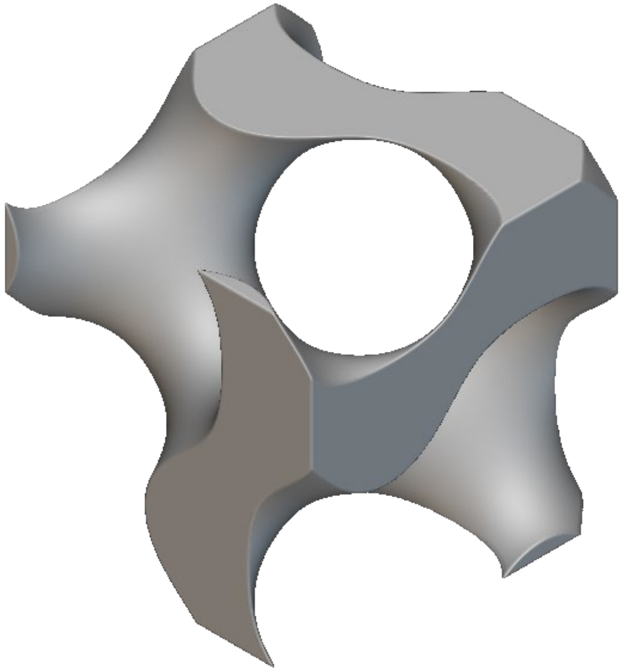

2 different unit cell size

2.5 mm and 4 mm

Design by nTopology software

FGPS

2.5 mm

4 mm

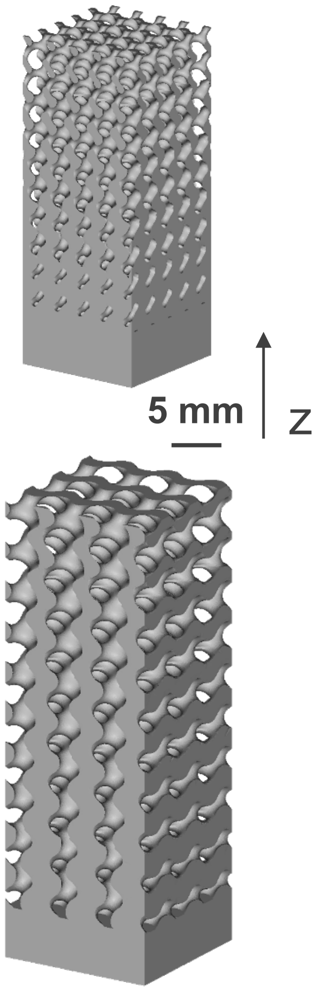

Relative density - dr (-)	Level constant t (-) **2.5 mm**	Level constant t (-) **4 mm**
0.17	-0.41	-0.66
0.34	-0.20	-0.32
0.50	0.00	0.00
0.66	0.20	0.32
0.83	0.41	0.66

2 TPMS unit cells for each density level along z axis

CoCo AM

Material

MATERIALS AND METHODS

Powder composition

Element	Mo	Al	Nb	Si	O	Ni	Fe
Weight %	14.6	2.8	2.8	0.3	0.11	0.004	Bal.

Laser Powder Bed Fusion (LPBF)

sisma

MySint 100 machine	
Building Volume	φ100x100mm
Laser Source	Fiber, 200W
Volume energy density	40 – 90 J/mm^3
Laser spot diameter	55 µm
Heated platform	NO
Scan Strategy	XY alternate

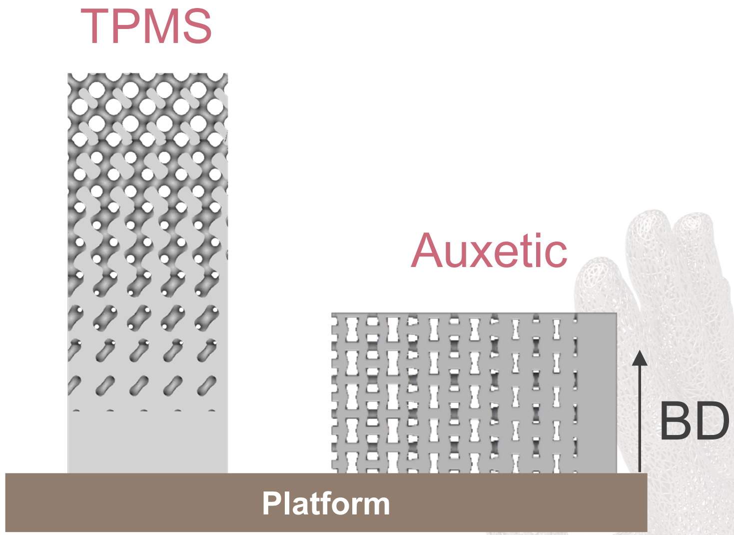

ADDITIVE 4 BIOMEDICAL

SC 09/A3 CoCo AM Additive Manufacturing

3D METROLOGY: AUXETIC

DESIGN

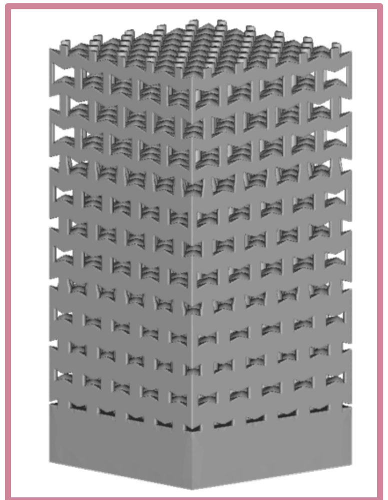

15°

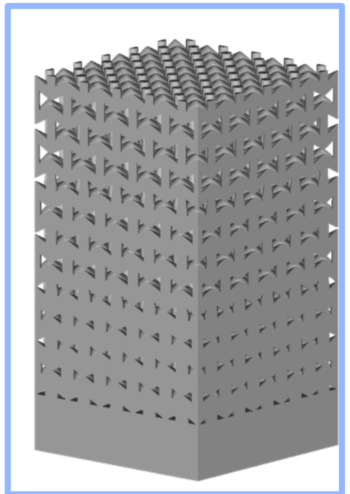

25°

LPBF

μ-CT image

15°

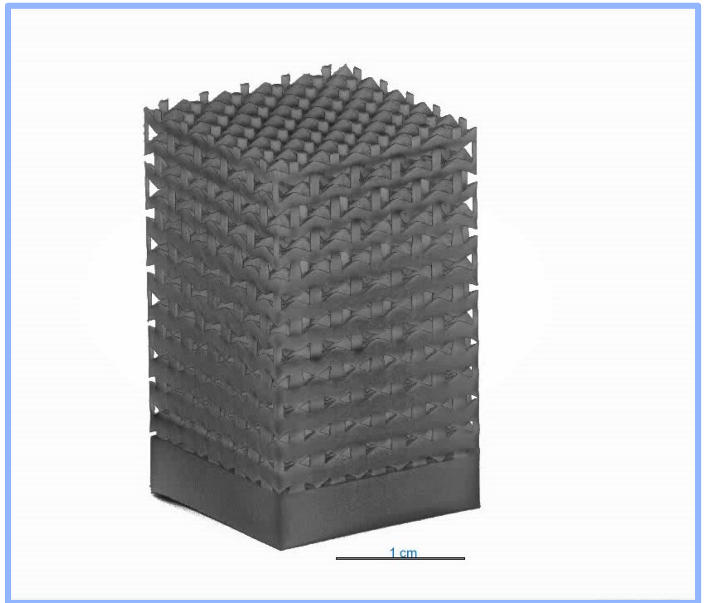

25°

Results

3D METROLOGY: TPMS

ADDITIVE 4 BIOMEDICAL

DESIGN

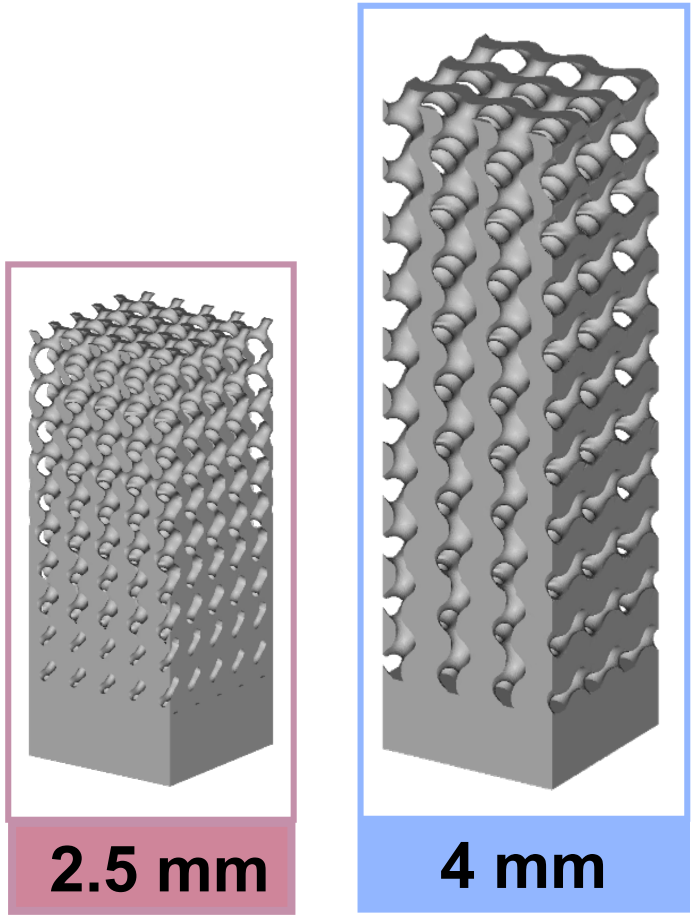

LPBF

μ-CT image

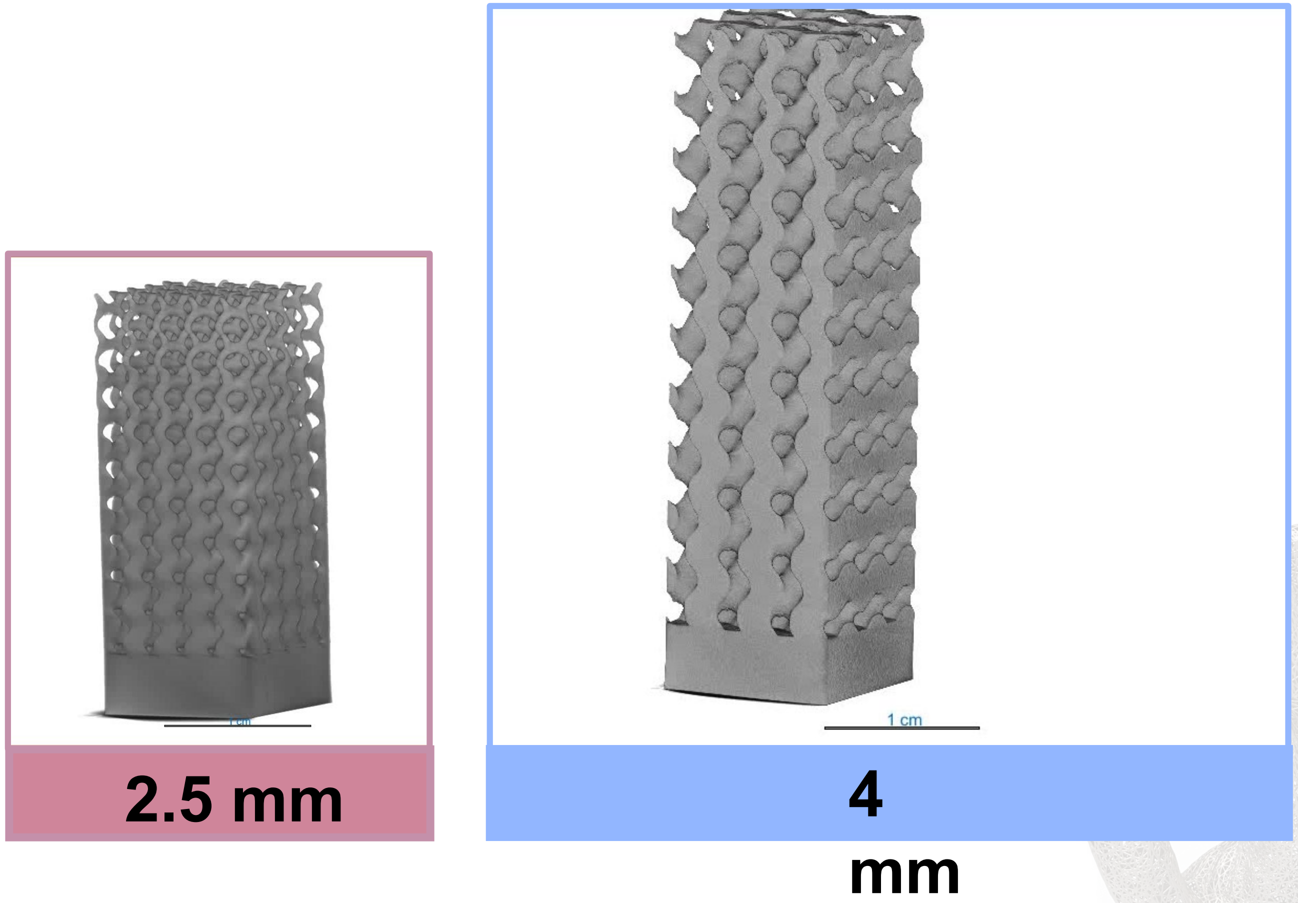

SC 09/A3 CoCo AM Additive Manufacturing

CAD VS. MICRO-CT

AUXETIC 15°

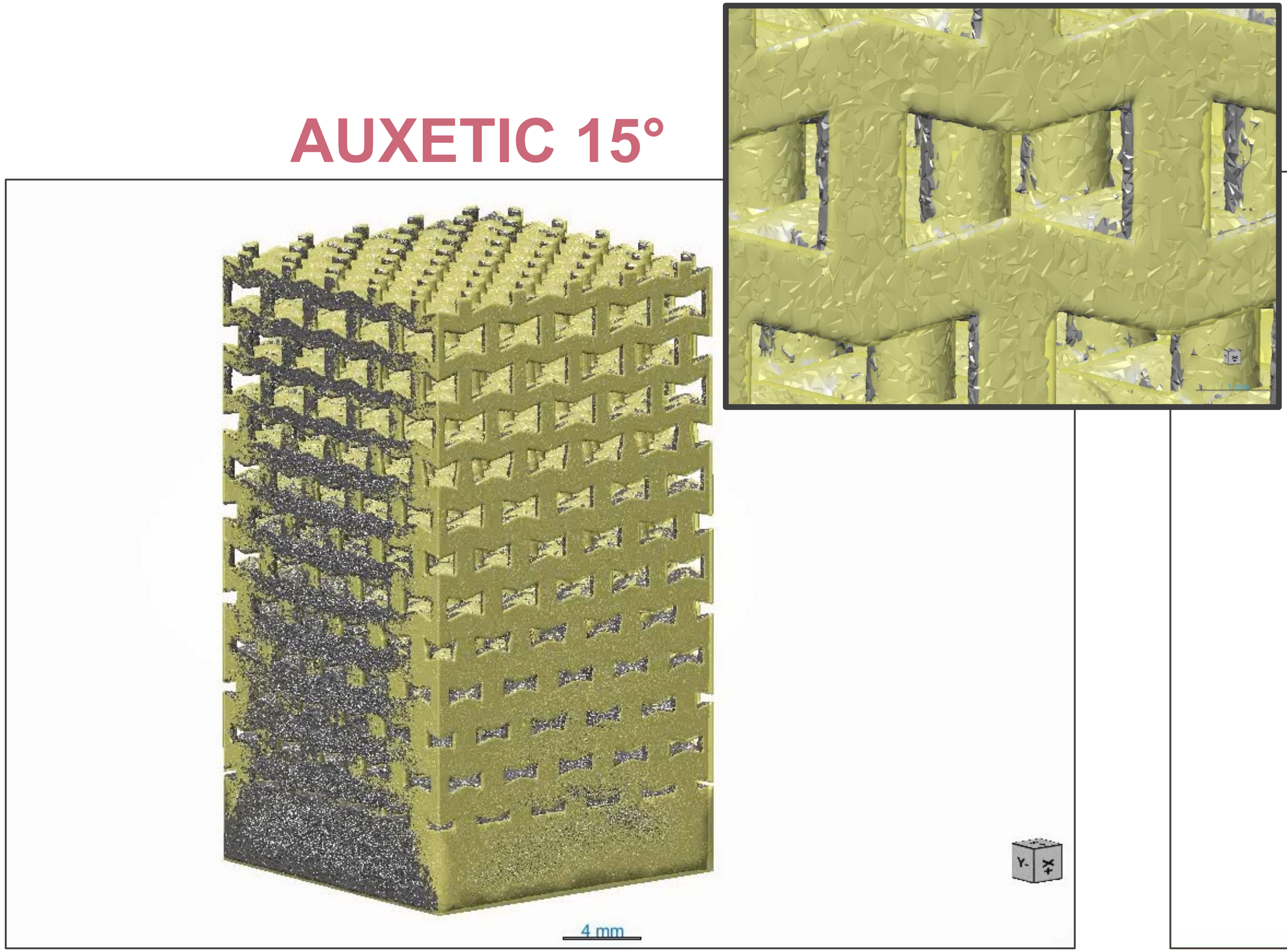

TPMS 4 mm

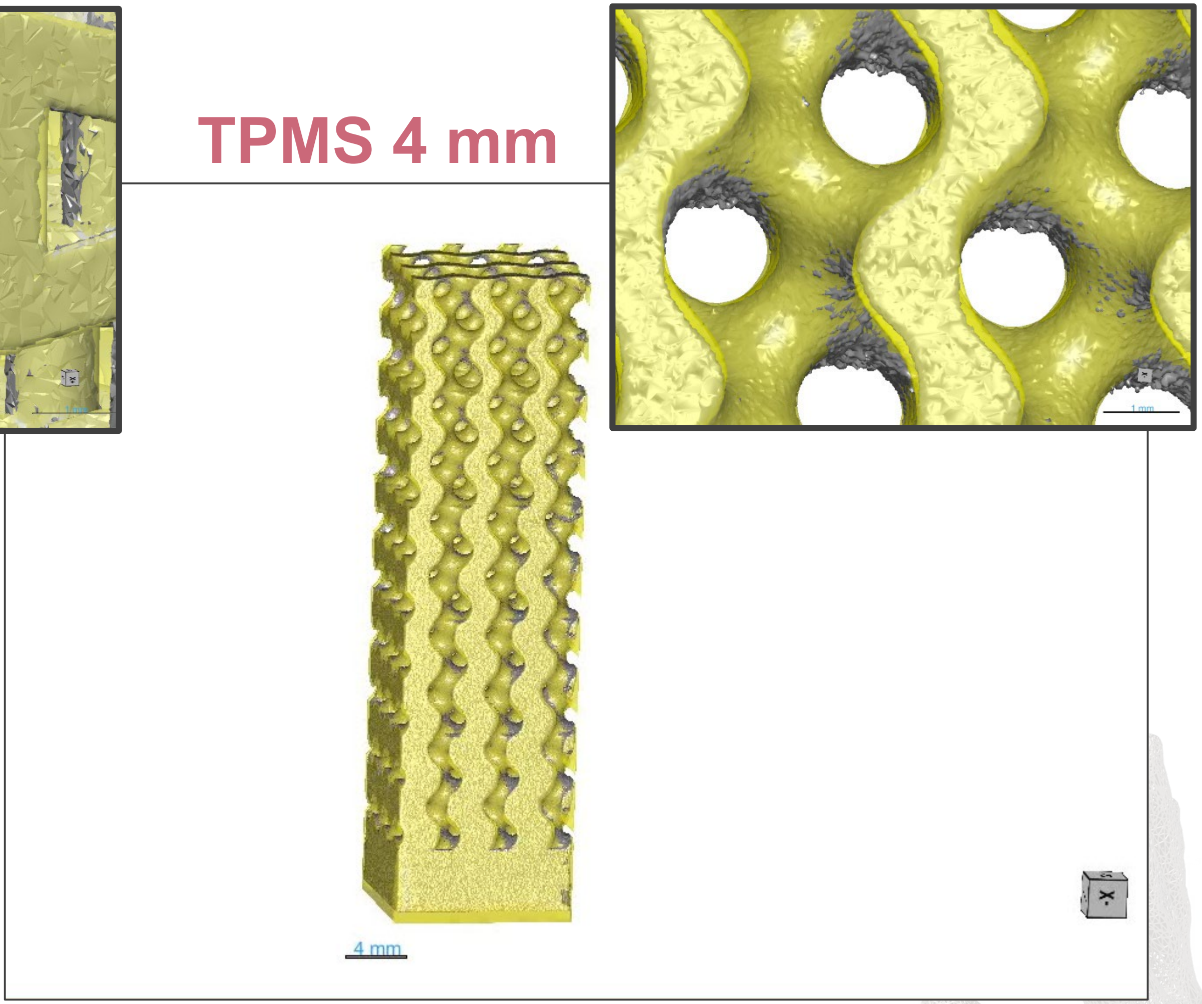

Overlap of CAD (yellow) with μ-CT (gray)

Results

CAD VS. MICRO-CT: AUXETIC

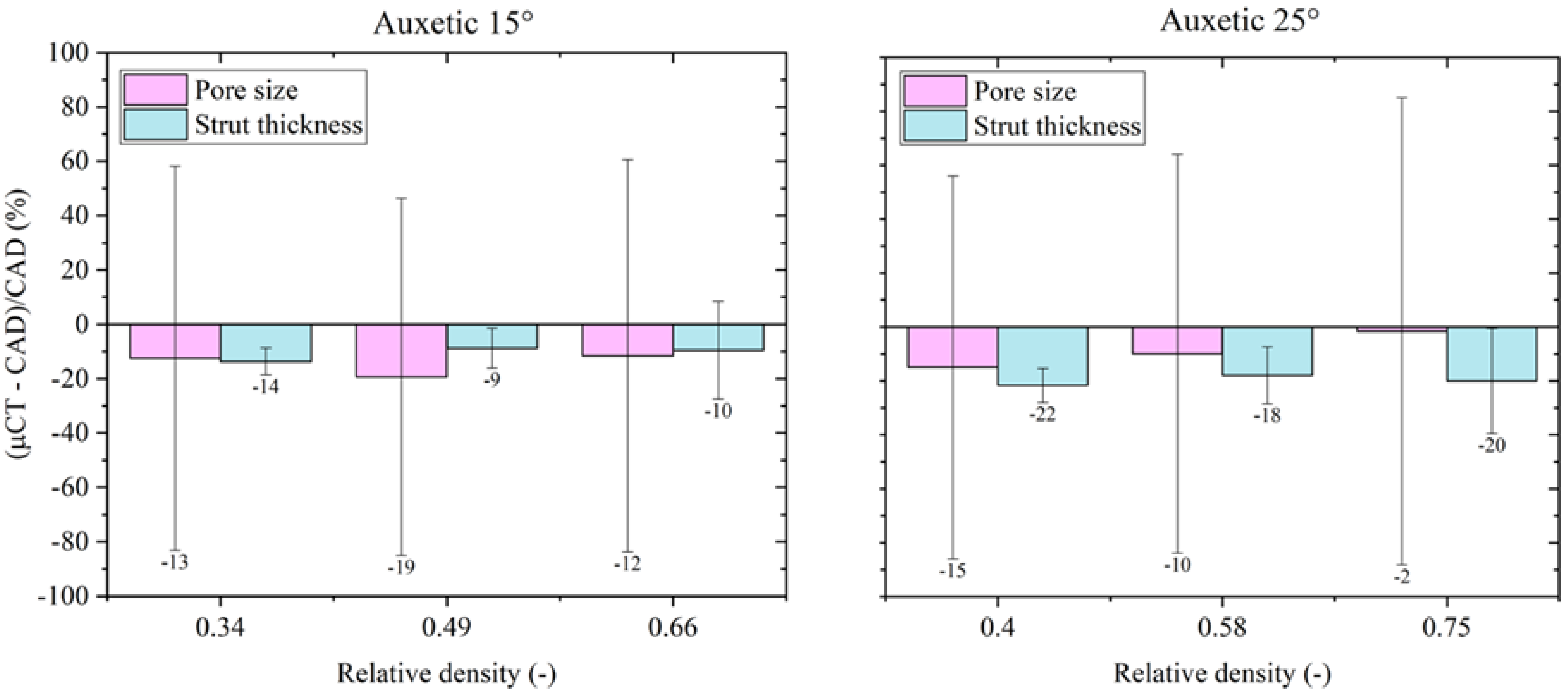

The undersizing of both the pore and the strut is associated with the surface irregularity of the structures. In detail, since both the strut and the pore were analyzed using the wall thickness method, the diameter of the sphere inscribed inside the pore is affected by the surface irregularity and the unmelted powder present on the struts differently from the strut thickness where the external unmelted powder does not affect the measure.

CAD vs. micro-CT: TPMS

Results

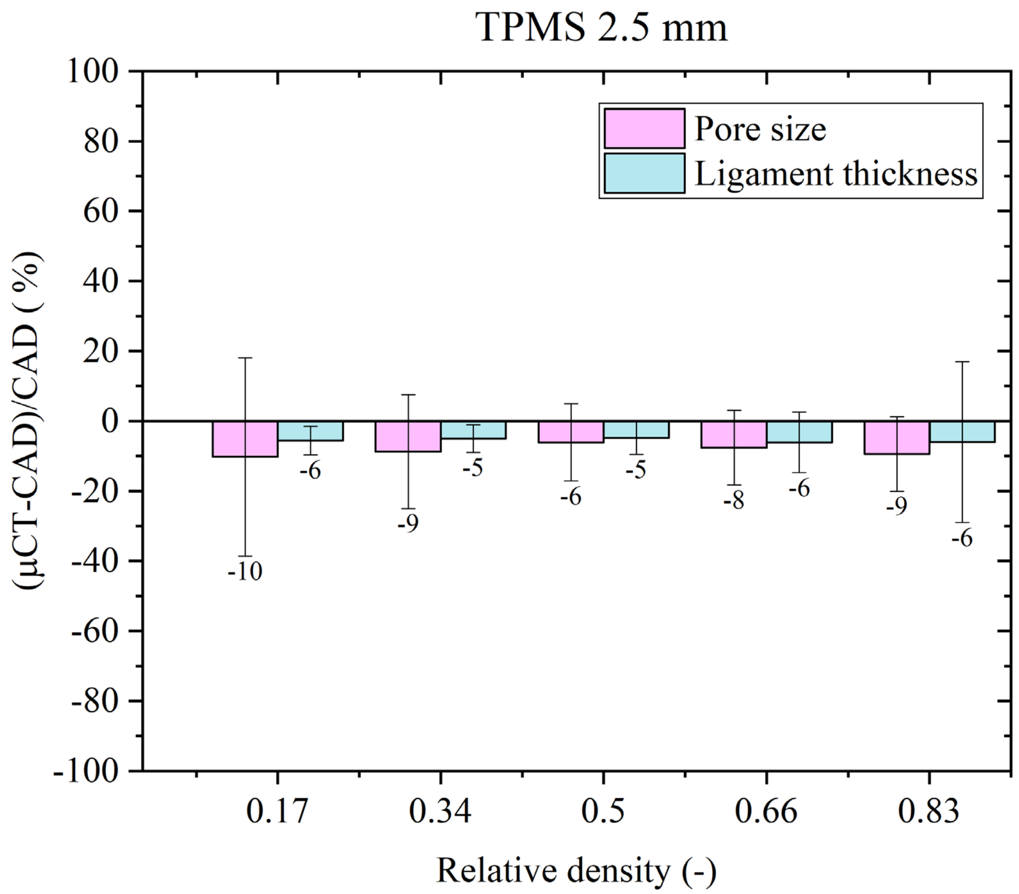

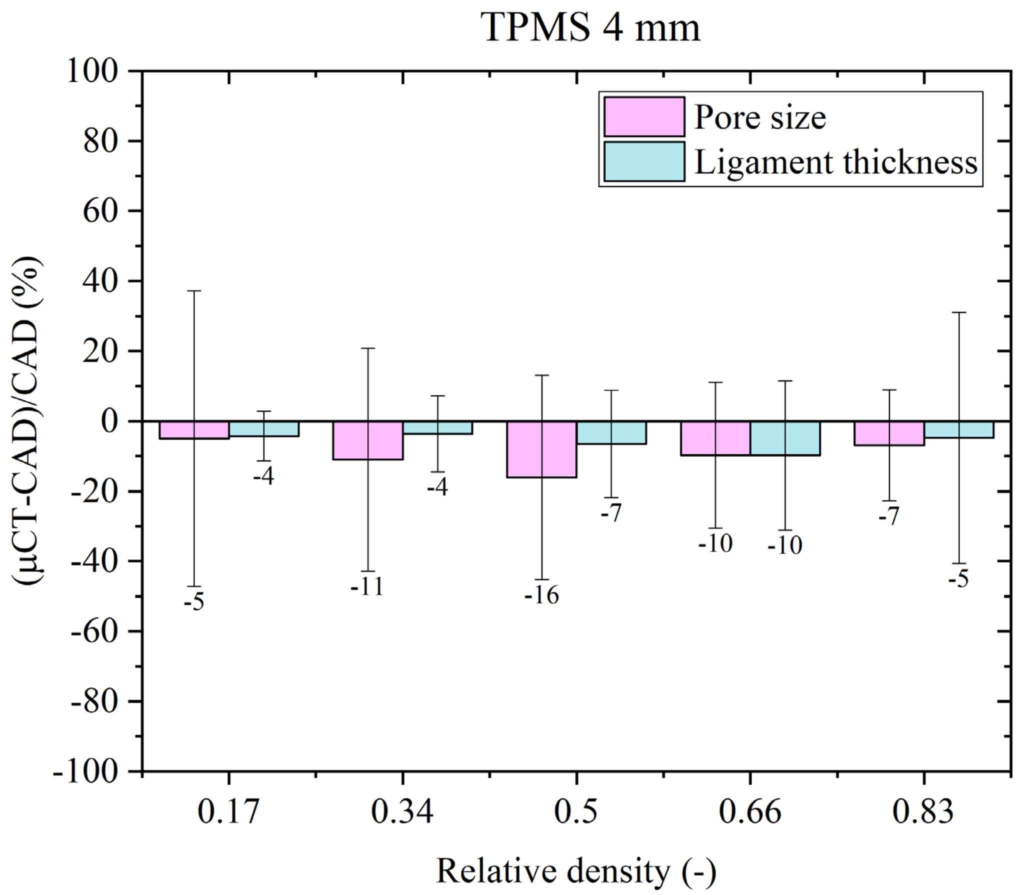

The undersizing of both the pore and the strut is associated with the surface irregularity of the structures. In detail, since both the strut and the pore were analyzed using the wall thickness method, the diameter of the sphere inscribed inside the pore is affected by the surface irregularity and the unmelted powder present on the struts differently from the strut thickness where the external unmelted powder does not affect the measure.

SC.09/A3 CoCo AM Additive Manufacturing

Results

MICROSTRUCTURAL CHARACTERIZATION

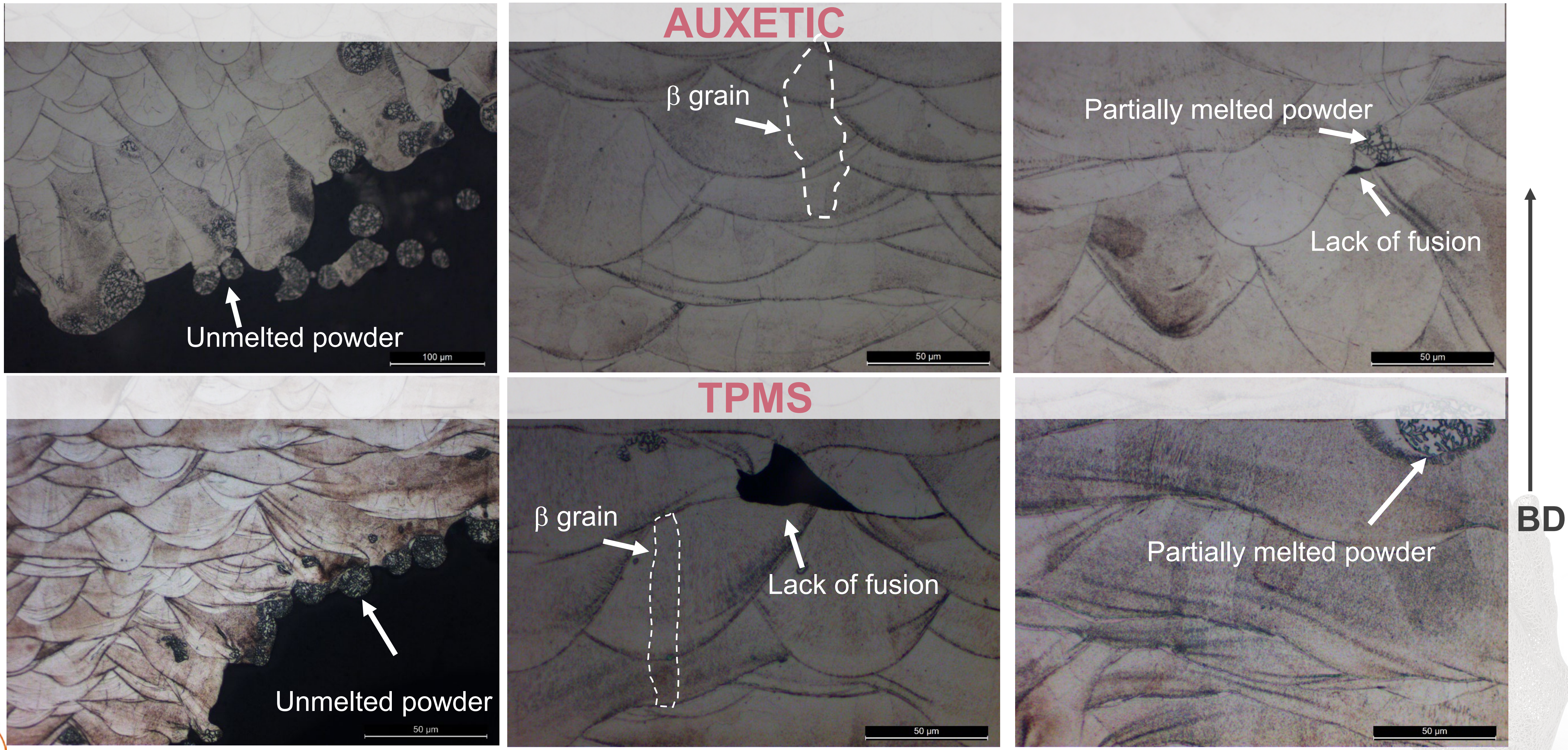

Results

MECHANICAL CHARACTERIZATION

ADDITIVE 4 BIOMEDICAL

Compression tests

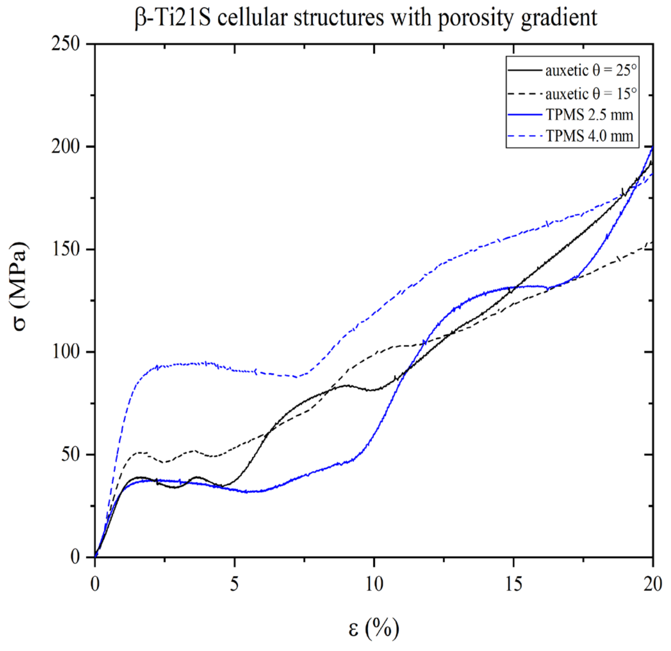

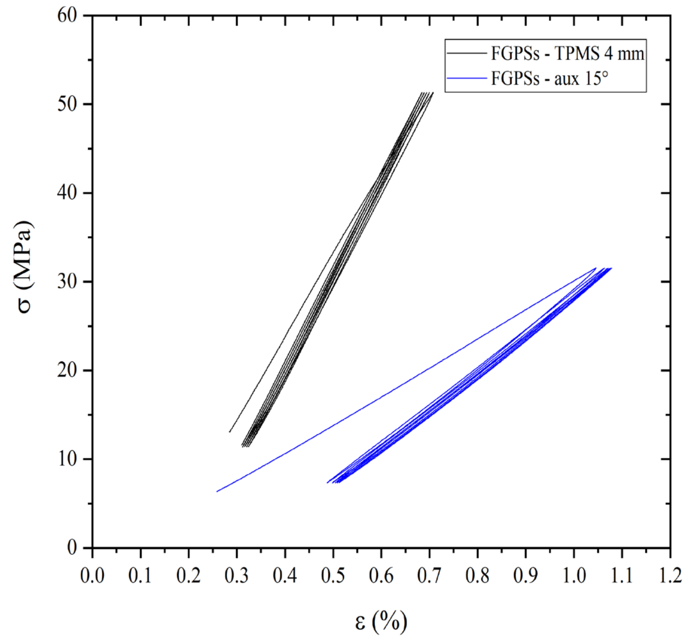

Simulation

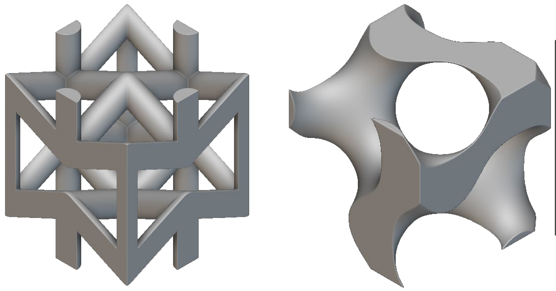

Homogenization method on single unit cell

+

$$\frac{1}{E} = \sum_{i=1}^{n} k_i \frac{1}{E_i}$$

Longitudinal FGPS results as a system with springs in series

FGPSs	$E_{quasi\text{-}elastic}$ (GPa)	σ_y (MPa)	**E_{cyclic} (GPa)**	**$E_{hom.\ nom}$ (GPa)**
Auxetic θ = 15°	3.8 ± 0.8	48.0 ± 1.3	**4.2 ± 0.1**	**4.88 (16%)**
Auxetic θ = 25°	3.2 ± 0.6	40.6 ± 0.6	**4.1 ± 0.1**	**5.24 (28%)**
TPMS 2.5 mm	3.5 ± 0.4	33.4 ± 0.4	**4.1 ± 0.1**	**4.55 (10%)**
TPMS 4.0 mm	*7.1 ± 0.2*	*84.3 ± 0.1*	*10.7 ± 0.1*	*4.19 (-61%)*

Too low number of unit cell along x and y (3 x 3) in the as-manufactured sample: boundary effect

SC 09/A3 CoCo AM Additive Manufacturing

Conclusions

Based on the idea to improve the connection between bone and femoral implant, the printability of the two different FGP cellular structures selected were evaluated:

- 3D metrology shows an undersize of both the pore size and strut thickness because of the surface irregularity and unmelted powder on the surface;
- From a manufacturability point of view, excellent results are obtained for all different FGPSs except for higher density level of auxetic θ equal to 25° due to loss of auxetic structure.
- A columnar structure along the building direction is evident and some partially melted powders are detected inside the material in all FGPSs.
- Simulation analysis permits to obtain very close results in term of stabilized elastic modulus except for the TPMS with 4 mm due to the boundary effect.

Lorena Emanuelli
lorena.emanuelli@unitn.it
INSTM- Operative center: University of Trento

UNIVERSITÀ DI TRENTO

THANKS FOR YOUR ATTENTION

"T-βone-Produzione additiva di protesi ortopediche a struttura trabecolare in lega di Ti-beta"

funded by the Fondazione Cariverona (Verona, Italy) Bando Ricerca e Sviluppo 2020

FONDAZIONE Cariverona